Available online at www.sciencedirect.com
SCIENCE DIRECT®
Journal of Power Sources 146 (2005) 804–808
JOURNAL OF POWER SOURCES
www.elsevier.com/locate/jpowsour

Investigation of lithium battery nanoelectrode arrays and their component nanobatteries

Fride Vullum [a], Dale Teeters [b,*]

[a] *Department of Chemical Engineering, The University of Tulsa, Tulsa, OK 74104, USA*
[b] *Department of Chemistry and Biochemistry, The University of Tulsa, 600 S. College Ave., Tulsa, OK 74104, USA*

Available online 31 May 2005

Abstract

Arrays of individual lithium nanobatteries were constructed using alumina membranes having pores 200 nm in diameters. These pores served as the "jackets" to hold a PEO-lithium triflate electrolyte. The pores were then capped with a cathode material consisting of an ambigel of V_2O_5 making arrays of individual nanobatteries. Cyclic voltammetry data indicated that a nanoelectrode array model could describe these arrays of cathodes. However, individual nanobatteries were further characterized by charge/discharge tests using atomic force microscopy cantilever tips to make electrical contact with the 200 nm cathodes of the nanobatteries. Average volumetric capacities of 45 $\mu Ah\,cm^{-2}\,\mu m^{-1}$ were recorded for these battery systems, demonstrating that these small lithium batteries could function as viable, miniaturized power sources for future nanodevices.

Keywords: Nanoelectrode arrays; Nanocells; Nanobatteries; Nanobattery arrays; V_2O_5; SnO_2

1. Introduction

If micro-electromechanical systems (MEMS), the proposed nanoelectromechanical systems (NEMS) and micro and nanosensors are to have even greater commercial importance, a self-contained power source is needed. Such capabilities have already been shown in work done by Pister and co-workers [1] on what he has termed "smart dust." These devices are small chips that contain completely autonomous sensing and communication platforms in millimeter volumes. They can be used for a distributed sensor network utilized to monitor environmental conditions. It is the microbattery contained on the smart dust chips that allows for the autonomous functioning of this novel device. One potential source of power on the micrometer and nanometer scale is the lithium battery. It is an excellent possibility that a miniaturized lithium system, i.e. a micro or nanobattery could provide the power needs of autonomous micro and nanodevices.

Thin-film rechargeable batteries with active layers of 1–10 μm have been of interest since the 1980s, and previous studies in the literature referring to micro or nanobatteries have dealt almost exclusively with thin film work [2–10]. In these studies, the actual size of the batteries, based on the electrode structure, was much greater than the nanometer scale. Recently, more work has been reported on making micro and nanobattery components and systems where nanoscale technology and assembly have been incorporated [11–18]. Our laboratory's recent work involves the fabrication of individual microbatteries [19], the development of tools for nanoscale characterization [19,20] and characterization of nanoscale components of micro and nanobatteries [19,21]. Our microbattery work was concerned with the construction of individual microbatteries made from 100 μm in diameter graphite particles as the anode, an electrolyte consisting of a polymer electrolyte confined in a nanoporous alumina membrane and numerous 200 nm V_2O_5 islands as the cathode. A conducting atomic force microscope cantilever tip was used to make contact with the 100 μm size graphite anodes so that charge and discharge studies could be done on these individual microbatteries [19].

* Corresponding author. Tel.: +1 918 6313147; fax: +1 918 6313404.
E-mail address: dale-teeters@utulsa.edu (D. Teeters).

0378-7753/$ – see front matter © 2005 Elsevier B.V. All rights reserved.
doi:10.1016/j.jpowsour.2005.03.086

The work that is presented here involves the fabrication and study of even smaller individual batteries, i.e. nanobatteries. In this case, the cathodes of an individual battery are 200 nm in diameter. The 200 nm cathodes cap the pores in nanoporous alumina membranes. The pores in the membranes are filled with a polymer electrolyte and the membranes are mounted on a sputter-deposited anode layer allowing each 200 nm cathode to perform as an individual nanobattery. Such a configuration of cells can be considered as a nanoelectrode array (NEA) of cathodes. In this work, we first studied the entire array of only the cathodes using a NEA model. If the NEA model is found to apply for this system, it will open the door to study arrays of nanobatteries as an ensemble of individual cells and lead to additional characterization options. However, we also wish to investigate the performance of individual nanobatteries. We will do this by using the tip of an AFM cantilever as the electrical contact on individual 200 nm cathodes and perform charge/discharge studies. As described previously, such miniature battery systems are of interest because they can be integrated into nanoscale systems where larger power sources simply would not fit. The array arrangement of these batteries may also make them useful for other application such as memory storage funtions. However, because of their extremely small scale, these systems also lend themselves to basic scientific investigation of such properties as the function of electrode materials.

2. Experimental

V_2O_5 sol–gel was made according to a method developed by Chaput et al. [22]. The alkoxide precursor vanadium (V) tri-*i*-propoxy oxide (Strem Chemicals, 98%) was hydrolyzed in a water/acetone solution and condensed to form a wet gel. The molar ratio generally used for the synthesis was 4/15/40 for the system $VO(OC_3H_7)_3/H_2O$/acetone. This gel was confined in the 200 nm pores of Al_2O_3 membranes (Whatman Anodisc filtration membranes) that were 13 mm in diameter and 60 μm thick. In order to make membranes for NEA studies, vanadium pentoxide wet gel was poured over the membrane and allowed to penetrate completely through the pores before gelation. Immediately after gelation, the membranes were transferred to an acetone bath and a total of eight solvent exchange steps were performed in order to remove most of the water in the gel. A second solvent exchange process was performed, where the acetone was removed by toluene distillation. This created a sufficiently small surface tension to maintain part of the porous network of the gel when dried at ambient pressure and temperature. The surface area of these porous V_2O_5 structures formed under ambient conditions (hence the name "ambigel") was analyzed using a Quantachrome Autosorb system. Ambigels with surface areas around 100–150 $m^2\ g^{-1}$ were consistently produced.

The membranes filled completely with V_2O_5 were studied by cyclic volatmmetry. Electrical contact to the membrane was made by sputtering the membrane with gold and then attaching the gold-coated side of the membrane to nickel foil using silver paste. The NEAs were studied by placing the nickel foil mounted membrane and two pieces of lithium ribbon (Aldrich 99.9%, 0.38 mm thick, 23 mm wide) into a propylene carbonate solution that was 1 M in lithium perchlorate (Ferro Corporation). Lithium served as both anode and reference electrode. For comparison, similar electrochemical tests were conducted on bulk gels. The bulk gel was prepared in the same manner as described above, except it was not put into membranes. It was crushed with a mortar and fixed to a nickel substrate with silver paste for cyclic voltammetry studies. All studies were done inside of an argon atmosphere glovebox. The gels were characterized by conducting cyclic voltammetry tests using an EG&G Princeton Applied Research model 273 potentiostat.

Individual nanobatteries were made by first sealing one side of 200 nm alumina membranes by coating the surface with nail polish. The viscous nail polish formed a surface coating that made an effective seal on this side of the membrane. Vanadium pentoxide wet gel was poured over the opposite side of the membrane and allowed to penetrate into the pores before gelation. However, because the pores were sealed with nail polish on the opposite side, the gel could not penetrate completely into the pores because of trapped air. A Joel JSM-35C scanning electron microscope with an energy depressive X-ray spectrometer (EDS) using an accelerating potential of 25 kV was used to analyze cross-sections. These studies indicated that the gel penetrated approximately 40 μm into the membranes. The membranes were then transferred to an acetone bath and subjected to the solvent exchange steps, which not only removed water in the gel, but also ensured complete removal of the nail polish coating. The second solvent exchange, using toluene, removed the acetone. Surface areas of these ambigels were approximately the same as ambigels used for NEAs.

The empty space in the pores was filled with a PEO wax electrolyte described previously [19] complexed with lithium triflate at a 15/1 ether oxygen to lithium ion ratio. This was accomplished by melting a small amount of wax onto the surface and leaving the membranes in a vacuum oven at 125 °C for 1–2 h. This process removed any air trapped in the pores, thereby allowing the molten wax to flow into the pore channel. The anode consisted of a 400 nm coating of tin oxide. This layer was formed by sputter coating, using a Cressington model 208HR sputter coater with a Manitou Systems PE-3 RF power supply. The tin oxide layer was deposited onto a nickel substrate, which served as a current collector. The anode was brought into intimate contact with the electrolyte by melting (approximately 110 °C) the excess wax on the surface of the cathode/electrolyte structure and placing the anode on top of this structure before it was allowed to cool. This completed the batteries. The batteries thus consisted of a continuous 400 nm thick anode layer on one side of a 60 μm thick nanoporous alumina membrane that was filled with approximately 20 μm of polymer electrolyte. The remaining volume of the pores (approximately 40 μm in thickness) was

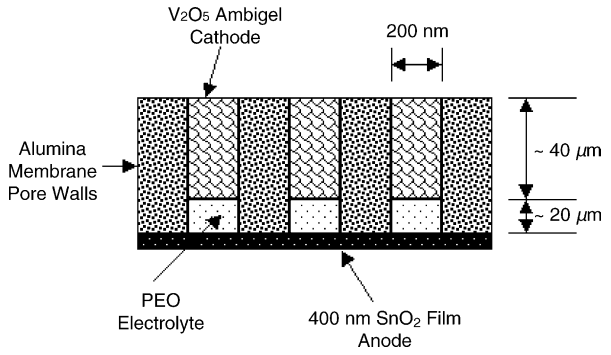

Fig. 1. Schematic of the nanobattery array configuration. Not to scale.

filled with V_2O_5, resulting in the top of the 200 nm pores being capped with this anode material. Fig. 1 is a schematic of the nanobattery configuration.

Fig. 2 shows an SEM image of the 200 nm pores before filling with the V_2O_5 and after the pores have been capped with the vanadia. Fortuitously it was found that any excess V_2O_5 ambigel could easily be "flaked off" the surface of the alumina membrane leaving pores that were capped level with the membrane surface. This resulted in individual, 200 nm batteries suitable for study. Most pores are completely filled, but a small number are not. Incomplete capping most likely resulted from improper sealing of the pores on the opposite side of the membrane or the actions of the solvent exchange process on the gel. As would be expected, pores that were not properly capped did not function well in the charge/discharge tests described next.

Individual naobatteries were characterized by running charge/discharge cycles with a Keithly Sub Femto Amp Remote Source Meter and the positioning capabilities of a Digital Instruments Nanoscope 3A atomic force microscope. The nanobattery arrays were placed on a nickel plate that served as a current collector. The current collector and the nanobattery arrays were positioned in the AFM and electrical contact was created by bring the cantilever tip of the atomic force microscope in contact with an individual cathode. In order to obtain electrical conduction with the silicon tip, it was first sputter coated with 20 nm of chrome followed by a sputter coating of 100 nm of gold. Electrical connections were made from the current collector and the AFM tip to the source meter completing the circuit.

3. Results and discussion

According to Jeoung et al. [23], previous work done with nanoelectrode ensembles (NEE) has shown that NEEs exhibit a scan rate dependence with three distinct voltammetric response regimes. At low scan rates, the NEE behaves as a planar macroelectrode, indicating linear diffusion. As the scan rate is increased, the current response is dominated by radial diffusion at the mouth of each pore. At even higher scan rates a "linear active" state is reached in which the diffusion is mainly linear diffusion within each individual pore. In the latter two cases, the nanoelectrodes are independent of each other and act as individual units [23].

Fig. 3 shows voltammograms of the gel in the pores of alumina membranes conducted at various scan rates. At low scan rates, the voltammograms are peak-shaped, indicating linear diffusion (see insert). At higher scan rates, the peaks become less apparent, which suggests an NEA mechanism.

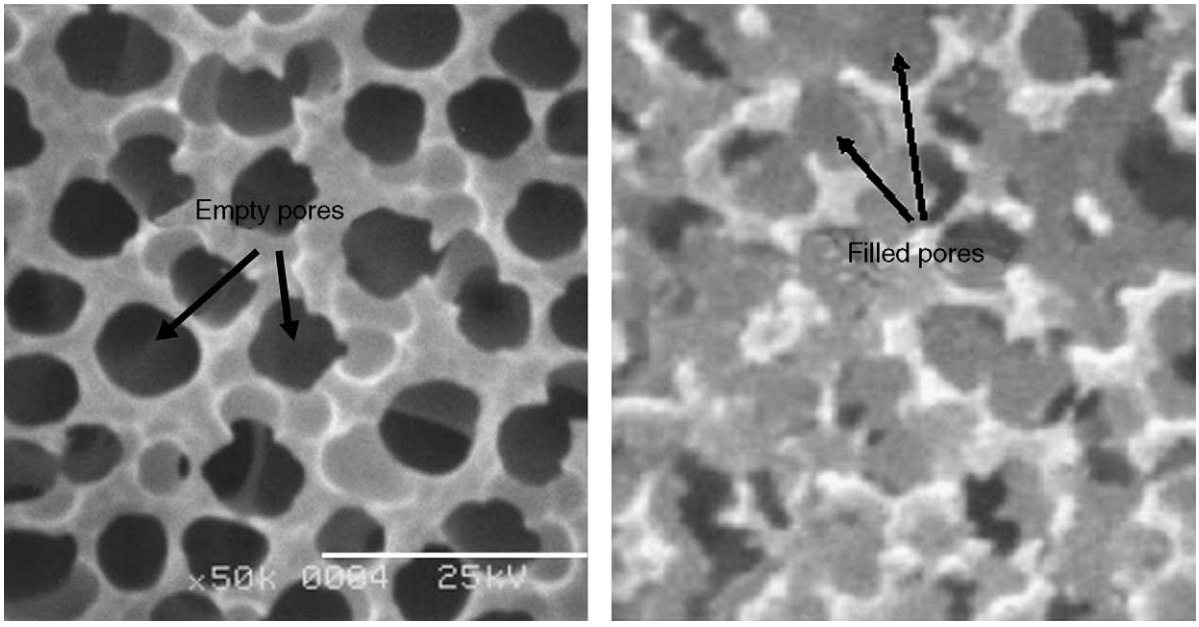

Fig. 2. SEM images of the alumina membrane with 200 nm pores. The empty membrane is shown to the left and the membrane after being capped with V_2O_5 gel is shown to the right.

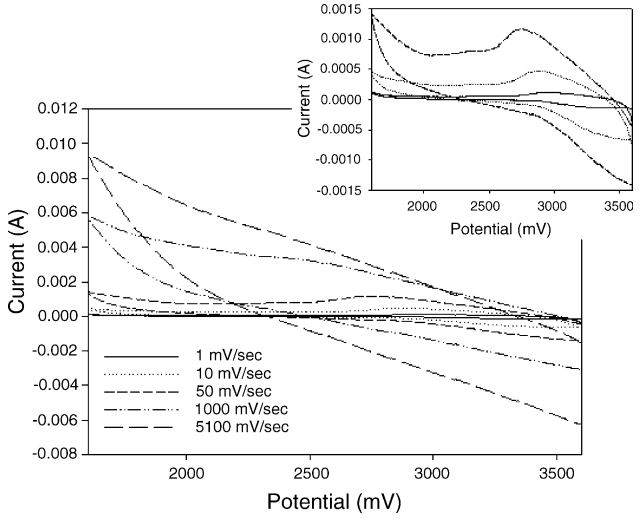

Fig. 3. Cyclic voltammograms of the V_2O_5 gel confined in an alumina membrane. The insert is the voltammograns for the slower scan speeds with an expanded scale so that their features can more clearly be seen.

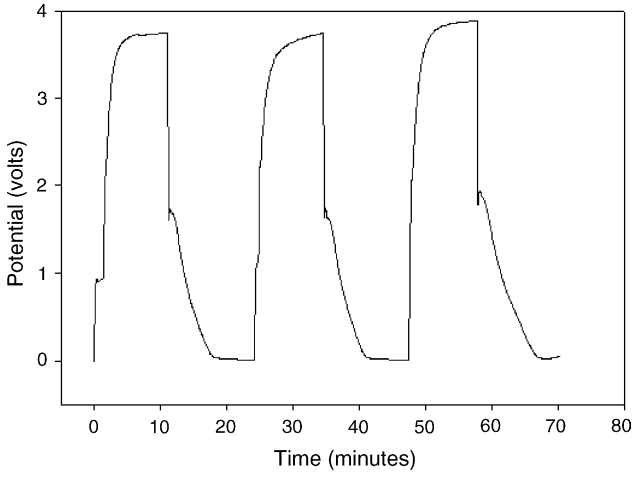

Fig. 4. Typical charge/discharge cycles for an individual nanobattery. The batteries were charged at a constant current of 50 pA and discharged at a constant current of 5 pA.

This is consistent with nonlinear diffusion, and mixed nonlinear and linear diffusion. The sigmoidal shape assumed by the voltammogram at the highest scan rate (5100 mV s^{-1}) is characteristic of basically all nonlinear diffusion, indicating that the individual pores act as independent nanocells. Intercalation experiments performed by Salloux et al. [24] with thin films of vanadium oxide aerogel have shown that Li can be inserted into vanadia gel at about 2.85 V. In that particular investigation the electrolyte was 1 M $LiClO_4$ dissolved in propylene carbonate, and the anode and the reference electrode were both elemental lithium, which is the same as in our experiment. It can be seen from Fig. 2 that the voltammograms show a peak at about 2.9 V, which indicates that lithium intercalation is occurring in our experiment as well.

For comparison, voltammograms for the ground bulk electrode were collected. These voltammograms (not shown here) show only a slight change in shape with varying scan rates indicating, as expected, a planer macroelectrode behavior. While no further analysis of data will be done in this preliminary study, cyclic voltammogram data indicate that these ensembles of cathodes can indeed be treated as a collection of nanocells and that we are inserting lithium into the arrays of V_2O_5 cathodes. The next data presented will investigate individual nanobatteries formed from these arrays.

The nanobattery arrays were fabricated as described in Section 2. The AFM tip was brought into contact with a selected V_2O_5 cathode cap and a 50 pA current was applied first in order to drive lithium ions from the electrolyte and insert them into each V_2O_5 ambigel cap. The nanobattery was then subjected to charge/discharge cycles, which consisted of charging at a rate of 50 pA until the potential reached its maximum value, which was around 3.75 V. Then the nanobatteries were discharged at a rate of 5 pA to values as low as 0.01 V. Several charge/discharge cycles are shown in Fig. 4. This discharge rate corresponds to a very large constant current density of 16 mA cm^{-2}. It seems reasonable that internal impedance of the cell could be responsible for the sharp ohmic voltage drop, i.e. IR drop at the beginning of the discharge. The cells may have a capacitance component as well. However, the large current density of the discharge step must also contribute to the sharp discharge profile.

The capacity of these nanobatteries was calculated by considering the size of the pores and the depth of penetration of the V_2O_5 gel into the membranes. The surface area of the cathodes was approximately 3.1×10^{-10} cm^2 and, as stated previously, the depth of penetration of the V_2O_5 into the pores was approximately 40 μm. Using the 5 pA discharge current, the capacities of the nanobatteries were calculated. As can be inferred from Fig. 4, the capacity of the nanobatteries remained relatively constant for each cycle at a value of approximately 45 μAh cm^{-2} μm^{-1}.

Our previous studies on microbattery systems, having anodes that were approximately 100 μm in diameter (the limiting electrode size) and, using V_2O_5 confined in nanopores, had volumetric capacities of 5 μAh cm^{-2} μm^{-1} [19]. The improvement in capacity could be due to several reasons. The SnO_2 anode's ability to store more lithium than graphite [25] could be responsible for higher capacities. In our previous study V_2O_5 xerogels of very low porosity were used as cathodes. The V_2O_5 ambigels used in this study have much higher porosities and surface areas that should improve performance. The improved porosity of the cathode and the utilization of true nanoscale cathodes for charging and discharging together must be important factors. These properties are no doubt beneficial since electrode components of this size and composition result in higher battery capacities, lower resistance, and lower susceptibility to slow electron-transfer kinetics than standard electrode configurations [11–15].

4. Conclusions

A technique was developed for constructing nanobatteries that have the potential for use in micro and nanosytems for a power source. An ambigel of V_2O_5 was placed in the 200 nm pores of alumina membrane, and cyclic voltammetry data indicated that arrays of these pores filled with V_2O_5 could be analyzed as a nanoelectrode array. Arrays of complete nanobatteries were made by coating the nanoporous alumina membranes on one side with a tin oxide layer that served as the anode. The 200 nm pores served as battery "jackets" since they were filled with a PEO-lithium triflate electrolyte and were also capped with V_2O_5 ambigel making an array of nanobatteries. In effect, nanobatteries of numerous parallel nanocells were made. An AFM cantilever was used to make contact with the V_2O_5 cathode caps. These nanobatteries were charged and discharged and had good capacities, proving that these small batteries could function as individual, minute power systems. Future work will involve addressing the fundamental properties and benefits of such nanopower sources.

Acknowledgments

The authors would like to acknowledge the Office of Naval Research and the National Science Foundation through grants EPS—0132354 and 9971534 for funding this work. One author (F.V.) would like to thank The University of Tulsa Graduate School for financial support.

References

[1] J.M. Kahn, R.H. Katz, K.S.J. Pister, Mobile networking for smart dust, in: Proceedings of the ACM/IEEE International Conference on Mobile Computing and Networking, Seatle, WA, August 17–19, 1999.
[2] J.B. Bates, G.R. Gruzalski, N.J. Dudney, C.F. Luck, X.-H. Yu, S.D. Jones, Solid State Technol. 36 (7) (1993) 59.
[3] L.G. Salmon, R.A. Barksdale, B.R. Beachem, R.M. LaFollette, J.N. Harb, J.d. Holladay, P.H. Humble, Development of rechargeable microbatteries for autonomous mems applications, in: Solid-State Sensor and Actuator Workshop, Transducer Research Foundation, Inc. Hilton Head, SC, 1998, pp. 338–341.
[4] K. Kinoshita, X. Song, J. Kim, M. Inaba, J. Kim, J. Power Sources 82 (1999) 170.
[5] Y.J. Park, K.S. Park, J.G. Kim, M.K. Kim, H.G. Kim, H.T. Chung, J. Power Sources 88 (2000) 250.
[6] Y.J. Park, J.G. Kim, M.K. Kim, H.G. Kim, H.T. Chung, Y. Park, J. Power Sources 87 (2000) 69.
[7] A. Levasseur, P. Vinatier, D. Gonbeau, Bull. Mater. Sci. 22 (1999) 607.
[8] K.S. Han, S. Tsurimoto, M. Yoshimura, Solid State Ionics 121 (1–4) (1999) 229.
[9] Y. Park, J.G. Kim, M.K. Kim, H.T. Chung, W.S. Um, M.H. Kim, H.G. Kim, J. Power Sources 76 (1998) 41.
[10] K. Kushida, K. Kuriyama, T. Nozaki, Appl. Phys. Lett. 81 (2002) 5066.
[11] N.C. Li, C.J. Patrissi, G.G. Che, C.R. Martin, J. Electrochem. Soc. 147 (2000) 2044.
[12] N.C. Li, C.R. Martin, B. Scrosati, Electrochem. Solid State Lett. 3 (2000) 316.
[13] V.M. Cepak, J.C. Hulteen, G. Che, K.B. Jirage, B.B. Lakshmi, E.R. Fisher, C.R. Martin, Chem. Mater. 9 (1997) 1065.
[14] C.J. Patrissi, C.R. Martin, J. Electrochem. Soc. 146 (1999) 3176.
[15] G.G. Che, B.B. Lakshmi, E.R. Fisher, C.R. Martin, Nature 393 (1998) 346.
[16] S.V. Batty, T. Richardson, F.B. Dias, J.P. Voss, P.V. Wright, G. Ungar, Thin Solid Films 284–285 (1996) 530.
[17] Y. Zheng, F.B. Dias, P.V. Wright, G. Ungar, D. Bhatt, S.V. Batty, T. Richardson, Electochim. Acta 43 (1998) 1633.
[18] J.H. Fendler, J. Disper. Sci. Tech. 20 (1999) 13.
[19] C. Dewan, D. Teeters, J. Power Sources C 119–121 (2003) 460.
[20] A. Layson, S. Gadad, D. Teeters, Electrochim. Acta 48 (2003) 2207.
[21] S. Vorrey, D. Teeters, Electrochim. Acta 48 (2003) 2137.
[22] F. Chaput, B. Dunn, P. Fuqua, K. Salloux, J. Non-Cryst. Solids 188 (1995) 11.
[23] E. Jeoung, T.H. Galow, J. Schotter, M. Bal, A. Ursache, M.T. Tuominen, C.M. Stafford, T.P. Russell, V.M. Rotello, Langmuir 17 (2001) 6396.
[24] K. Salloux, F. Chaput, H.P. Wong, B. Dunn, M.W. Breiter, J. Electrochem. Soc. 142 (1995) L191.
[25] Y. Idota, T. Kubota, A. Matsufuji, Y. Maekawa, T. Miyasaka, Science 276 (1997) 1395.